

Variable Structure Systems Theory in Training of Radial Basis Function Neurocontrollers – Part II: Applications

Mehmet Önder Efe
Carnegie Mellon University
Electrical and Computer Engineering Department
Pittsburgh, PA15213-3890, U.S.A.
efemond@andrew.cmu.edu

Abstract – Some illustrative applications of Variable Structure Systems (VSS) theory based parameter tuning in control systems are presented in this paper. The underlying idea of robustness against disturbances and high tracking performance is observed through an appropriate integration of Radial Basis Function Neural Networks (RBFNN) and VSS based training scheme. The examples presented include the control of mechatronic systems, biochemical processes and a chaotic system named Duffing oscillator.

Keywords: Sliding Mode Control, Parameter Tuning, Neural Networks

I. INTRODUCTION

VSS theory is well known with its robustness to the disturbances e.g. noise on the observed quantities and uncertainties entering the system through control channels [1]. The widespread variable structure controller design methodology prescribes that the behavior in the phase space would be composed of two phases: namely the reaching mode and the sliding mode. The approach is basically a two-sided decision mechanism, which is strictly dependent upon the value of a measured quantity called ‘switching function’. It is obvious that the control signal is extremely vulnerable to the measurement noise as it affects the value of switching function, which is very close to zero during the sliding mode. The apparent consequence of this is the well-known problem of ‘chattering’ [2].

Being not limited to what is mentioned above, the standard method requires the availability of the nominal system together with the bounds of the uncertainties.

This paper demonstrates the applications of the approach discussed in [3], which is applicable without knowing the analytical details of the plant to be controlled. The most substantial contribution of [1] is the fact that the error on the control signal is constructed and this has enabled the designers to train the intelligent controller, which may be a neural network or a fuzzy system. Basically, the system under control is assumed to be in the class given below.

$$\theta_i^{(r_i)} = f_{p_i}(\underline{\theta}) + \sum_{j=1}^n d_{ij} \tau_j \quad i = 1, 2, \dots, n \quad (1)$$

where, $\underline{\theta}$, $\underline{\tau}$ and D are the state vector, input vector and the input gain matrix respectively. The system is in an ordinary feedback loop [3], and the switching function for i^{th} subsystem is defined as in (2), in which λ_i is a strictly positive scalar.

$$s_{p_i}(e_i) = \left(\frac{d}{dt} + \lambda_i \right)^{r_i-1} e_i \quad (2)$$

Based on these, the error at the output of the controller is formulated as in (3) [3].

$$\underline{s}_c = (GD)^{-1} \left(\dot{\underline{s}}_p + \xi \operatorname{sgn}(\underline{s}_p) \right) = \underline{\tau} - \underline{\tau}_d \quad (3)$$

where $\underline{s}_p(e) = G\underline{e} = G(\underline{\theta} - \underline{\theta}_d)$ and ξ is a positive definite diagonal matrix of dimension $n \times n$.

In the second section some application specific issues are presented. The third section demonstrated the simulation results for a double pendulum system, the fourth section discusses the control of a Continuously Stirred Tank Reactor (CSTR) and the fifth section focuses on the control of a Duffing oscillator. The conclusions constitute the last part of the paper.

II. PRACTICAL ISSUES

The analysis and the design approach presented [3] have tried to illuminate the Sliding Mode Control (SMC) problem from a theoretical perspective. In this subsection, we discuss several issues related to the practical applications of the discussed methodology.

A. Chattering

Since the control decision during the sliding mode is tightly dependent to the sign of a measured quantity being noisy and very close to zero, the decision along the sliding manifold exhibits sensitivity to noise on the observations. Among many alternatives available [1-2,4], a common approach to eliminate the chattering is to smooth the sign function, which corresponds to introduce a boundary layer [2]. In this paper, we adopt the following approximation for the $\operatorname{sgn}(\cdot)$ function.

$$\text{sgn}(x) \equiv \frac{x}{|x| + \delta} \quad (4)$$

where δ determines the sharpness around the origin. Since the function in (4) is not discontinuous at the origin, the decision mechanism softly switches around the vicinity of the decision surface.

B. Actuation Speed

Another important issue is the actuation speed of the system under control, i.e. the ability to respond to what is imposed timely. Since we do not assume that the details concerning the dynamic model of the system are unavailable, what causes a difficulty from a practical point of view is the selection of the matrix ξ , which characterizes the behavior during the reaching mode. The values of this quantity can only be set by trial-and-error due to the lack of system-specific details.

C. Obtaining the Equivalent Error from the Observed Data

Lastly in this subsection, we focus on the construction of the \underline{s}_c of (3), which requires the differentiation of \underline{s}_p . What we adopt in this paper is to filter the measured values of \underline{s}_p and differentiate afterwards. Denote S as the Laplace variable, and use the linear system given as

$$H(S) = \frac{\alpha S}{Q(S)} \quad (6)$$

where $Q(0) = \alpha > 0$ and $\text{Real}\{\text{roots}(Q(S))\} < 0$. The order of the denominator polynomial and the locations of the roots are left to the designer, because these issues require several trials to refine the selections and are subject to the application together with its operating environment.

Lastly, it should be noted that the cost of the information loss by using such a filter, whose input is \underline{s}_p and output is an estimate of $\dot{\underline{s}}_p$, is a matter of how robust the devised control algorithm is. More explicitly, the separation of the noise and the actual value of \underline{s}_p leads to a corruption on \underline{s}_p , and when differentiated afterwards, some valuable information is lost together with the elimination of the noise component. Here we assume that mentioned loss causes an uncertainty, which enters the system through the control channels, and which is particularly effective during the sliding mode; and this uncertainty can be alleviated if it falls within the limits allowing the maintenance of the invariance during the sliding mode [1].

In the remaining part of the paper, three application examples are presented. In order to demonstrate the applicability of the developed scheme, the examples focus on the control of mechatronic systems, biochemical processes, and chaotic

systems. Some common points that should here be highlighted for the following three sections are as follows: we tune solely the weight parameters of the neurocontrollers and we set these parameters initially to zero, i.e. the parametric evolution starts from the origin. The noise sequences are Gaussians having zero mean, and the adopted filter structure has the structure given in (6). Furthermore, we set $\delta=0.25$ in all examples.

$$H(S) = \frac{\alpha S}{Q(S)} = \frac{\alpha S}{S^2 + 2\sqrt{\alpha}S + \alpha} \quad (6)$$

III. SMC OF A DOUBLE PENDULUM

The differential equations characterizing the behavior of the system are given in (7)-(8), in which the angular positions and the angular velocities for each pendulum define the state vector. The control inputs, which are denoted by τ_1 and τ_2 , are provided to the relevant pendulum by servomotors at the base. The parameters of the plant are given in Table I.

$$\ddot{\theta}_1 = \left(\frac{M_1 g r}{J_1} - \frac{k_s r^2}{4J_1} \right) \sin(\theta_1) + \frac{k_s r}{2J_1} (l-b) + \frac{\tau_1}{J_1} + \frac{k_s r^2}{4J_1} \sin(\dot{\theta}_2) \quad (7)$$

$$\ddot{\theta}_2 = \left(\frac{M_2 g r}{J_2} - \frac{k_s r^2}{4J_2} \right) \sin(\theta_2) - \frac{k_s r}{2J_2} (l-b) + \frac{\tau_2}{J_2} + \frac{k_s r^2}{4J_2} \sin(\dot{\theta}_1) \quad (8)$$

where, $g=9.81 \text{ m/s}^2$ is the gravitational acceleration constant. As given in Table I, since $b < l$, the two pendulums repel each other in the upright position. The model introduced in this section has been studied by Spooner and Passino [4], who discuss the decentralized adaptive control using RBFNN.

Under the conditions given in the second row of Table II, in response to a sinusoidal reference vector, the state response and the error response are obtained as illustrated in Figures 1 and 2 respectively. The control signals leading to this response are illustrated in the top row of Figure 3, and the behaviors in the phase spaces are depicted in the bottom row of Figure 3. Clearly the smoothness of the control signal and the behavior in the phase space recommend the use of the approach presented in mechatronics. Lastly, the evolutions in the parameters of the two RBFNN controllers (ϕ) are illustrated in Figure 4, from which the bounded evolution is clear.

IV. SMC OF A BIOCHEMICAL PROCESS

Chemical process engineering is another application field utilizing the techniques of control engineering expertise. In this subsection, we consider the dynamic model of a CSTR discussed in [5], which illustrate the SMC task with Gaussian networks and wavelet networks. The governing equations of

the process dynamics are as described below, and the parameters are defined in Table III.

$$\dot{\theta}_1 = -\theta_1 + Da(1-\theta_1)\exp\left(\frac{\theta_2}{1+\frac{\theta_1}{\gamma}}\right) \quad (9)$$

$$\dot{\theta}_2 = -\theta_2 + T_R Da(1-\theta_1)\exp\left(\frac{\theta_2}{1+\frac{\theta_1}{\gamma}}\right) - \beta(\theta_2 - \theta_c) + \eta \quad (10)$$

The control problem is to enforce the dimensionless concentration (θ_1) to follow a desired trajectory by altering the dimensionless coolant temperature (θ_c). During the control operation, the second state, which is the dimensionless temperature (θ_2), is constrained to evolve boundedly in time. In [4], the nominal operating point of the CSTR system is described as $\theta_1=0.4126$, $\theta_2=3.28$ and $\theta_c=3.04$, the state values among which are used as the initial state values in this paper. According to the simulation settings given in the third column of Table II, one should notice from the first row that the controller uses solely the noise corrupted tracking error information in synthesizing the necessary control sequence. In Figure 5, the desired and the observed states are illustrated. In the bottom right subplot of this figure, the error is seen. At time $t=3200\text{sec}$, a step change occurs in the reference trajectory, which is also studied by Knapp et al [4], and the system successfully follows the imposed trajectory. It must be noted that since the system under control is of first order, the sliding surface of the conventional design becomes a point in the single dimensional error space, and this point corresponds to the origin. Consequently, the problem does not require a λ selection. In the top left subplot of Figure 6, the applied control signal (θ_c) is illustrated. This subplot reveals that the control signal has a sufficiently smooth characteristic after the transient phase. The remaining three subplots in Figure 6 depict the time evolution of the adjustable neurocontroller parameters. These subplots confirm the evolution in finite volume claim of [3]. The variables seen in Figures 5 and 6 have been redrawn in Figures 7 and 8 with the same graphical allocation but around $t=3200\text{sec}$, at which a step change occurs in the command signal. When compared to the results discussed in [5], it can be said that the settling time is not as small as in [5], but the computational simplicity, i.e. the number of neurons, and acceptable tracking accuracy make the approach presented a good alternative for control of chemical processes.

V. SMC OF A CHAOTIC SYSTEM

Understanding the chaotic behavior has constituted a challenge for years as the outputs from which represent the

entire richness of nonlinear phenomena during the course of even the finite-time observations. The behavioral diversity in chaos is therefore attributed to its deterministic unpredictability or the unpredictable determinism, which exists in the nature of the system. Furthermore, sensitive dependence to the initial conditions makes the chaotic systems attractive test beds to test the performance of novel control algorithms. In this section, we discuss the Duffing system studied in [6], which illustrates the identification and control issues for a number of chaotic systems. The differential equation governing the dynamics of the system is given as follows:

$$\ddot{\theta} = -p_1\theta - p_2\theta^3 - p\dot{\theta} + q\cos(\omega_d t) + \tau \quad (11)$$

where, $p_1 = 1.1$, $p_2 = 1$, $p = 0.4$, $q = 2.1$ and $\omega_d = 1.8$. The control problem is to enforce the states to the periodic orbit described as follows:

$$\ddot{\theta}_d = -\sin(\theta_d) \quad (12)$$

with $\theta_d(0) = 1$ and $\dot{\theta}_d(0) = 0$. The simulation data for this example is given in the fourth column of Table II. In the left subplots of Figure 9, the reference θ trajectory, the response of the system and the tracking error are illustrated respectively. The same quantities for the second state are figured in the right subplots. Clearly, the response of the system converges to the desired trajectories in a short while. In Figure 10, the control activity, which is admissibly smooth despite the presence of noise sequence, leading to the obtained state behavior is shown. The motion in the phase space is depicted in the top right subplot of Figure 10, in which the error vector hits the sliding line and approximately after $t = 0.25$ sec starts moving towards the origin as characterized by the locus along the sliding line. The response of the system is drawn in the bottom subplot of Figure 10, which apparently confirms the accurate tracking claim of the approach. Lastly, the parametric evolution is shown in Figure 11, from which the bounded evolution is apparent.

VI. CONCLUSIONS

A SMC based parameter tuning strategy is discussed in [3]. This paper has illustrated some application examples of the strategy. In all of the examples, the results are highly promising for control engineering practice. A last desirable characteristic of the approach is its simplicity in terms of the computational requirements. More precisely double pendulum example costs 2×452 floating point operations (flops), CSTR example costs 143 flops and Duffing oscillator example costs 452 flops for a single forward pass for output evaluation and a backward pass for parameter tuning with the proposed scheme. A detailed view of the cost is illustrated in

Figure 12. In the view of what have been observed, the algorithm discussed yields a good performance for control of unknown systems belonging to class given by (1).

REFERENCES

- [1] Hung, J. Y., Gao, W. and Hung, J. C., "Variable Structure Control: A survey," *IEEE Trans. on Industrial Electronics*, Vol. 40, No. 1, pp.1-9, February 1993.
- [2] Slotine, J. J. E. and Li, W., *Applied Nonlinear Control*, Englewood Cliffs, NJ: Prentice-Hall 1991.
- [3] Efe, M. O., "Variable Structure Systems Theory in Training of Radial Basis Function Neurocontrollers - Part I: Theoretical Foundations," *Proc. of the 2001 NATO ASI on Neural Networks for Instrumentation, Measurement, and Related Industrial Applications: Study Cases (NIMIA-SC 2001)*, Oct. 9-20, Crema, Italy, 2001.
- [4] Spooner, J. T. and K. M. Passino, "Decentralized Adaptive Control of Nonlinear Systems Using Radial Basis Neural Networks," *IEEE Trans. on Automatic Control*, Vol. 44, No.11, pp. 2050-2057, 1999.
- [5] Knapp, T. D., H. M. Budman and G. Broderick, "Adaptive Control of a CSTR with Neural Network Model," *Journal of Process Control*, Vol. 11, pp. 53-68, 2001.
- [6] Poznyak, A. S., W. Yu and E. N. Sanchez, "Identification and Control of Unknown Chaotic Systems via Dynamic Neural Networks," *IEEE Trans. on Circuits and Systems-I: Fundamental Theory and Applications*, Vol. 46, No. 12, pp. 1491-1495, December 1999.

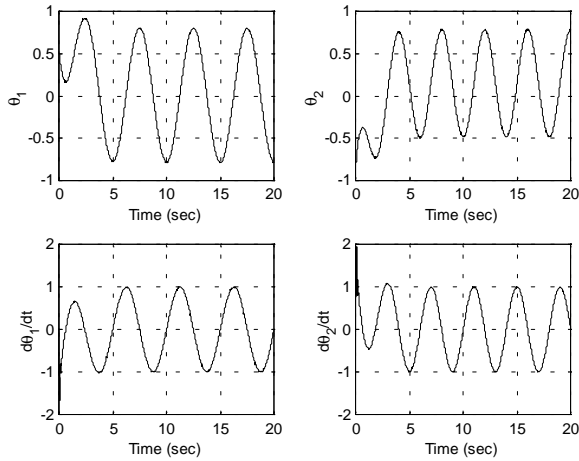


Figure 1. Response of the double pendulum system

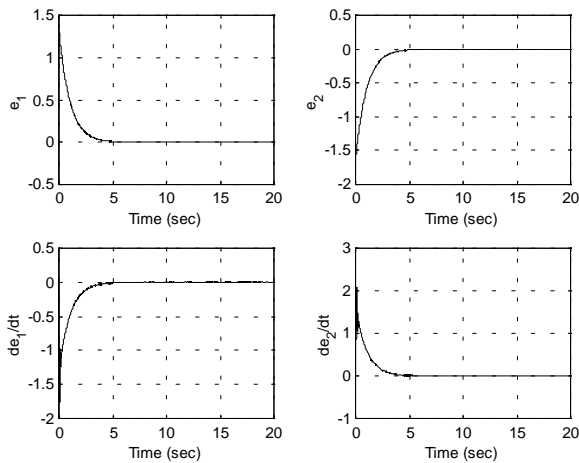


Figure 2. Behavior of the state tracking errors

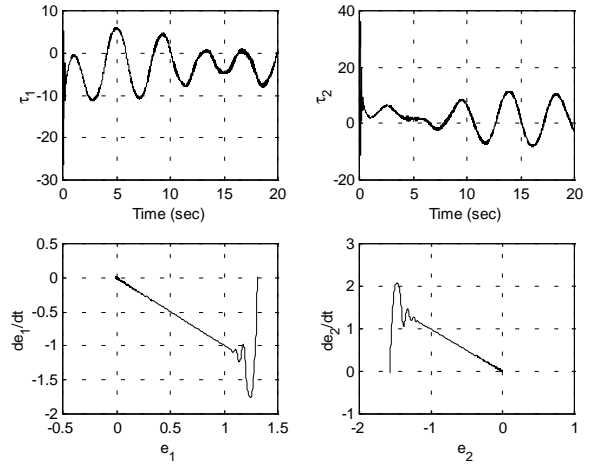


Figure 3. Applied torque signals and the behavior in the phase space

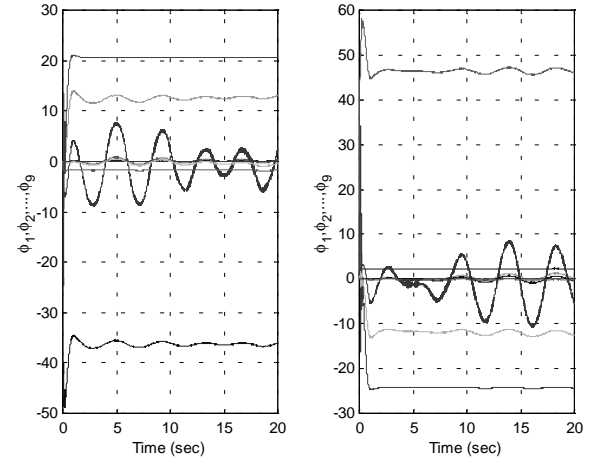


Figure 4. Time evolution of the parameters of the two controllers

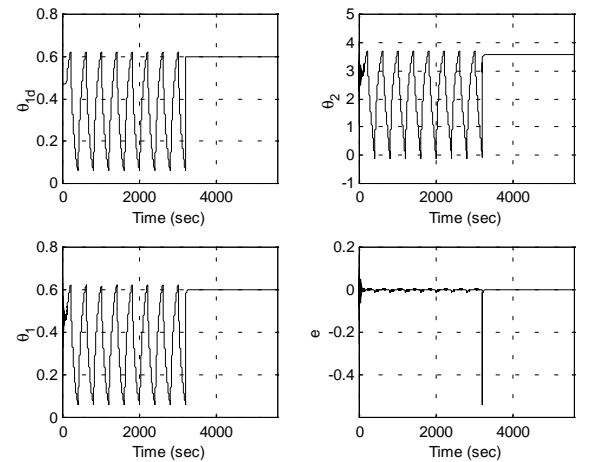


Figure 5. Desired and observed states with error signal in CSTR control example

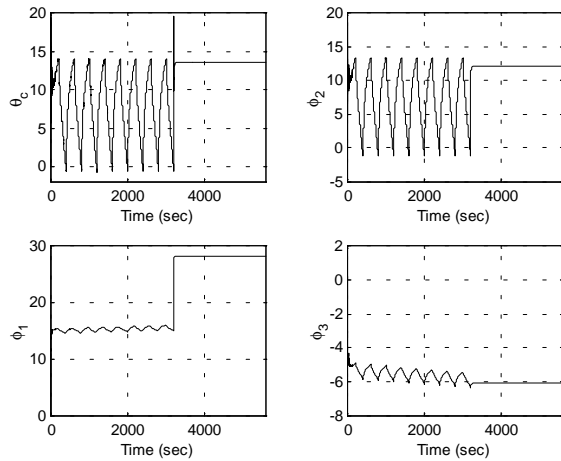


Figure 6. Control signal and parametric evolution

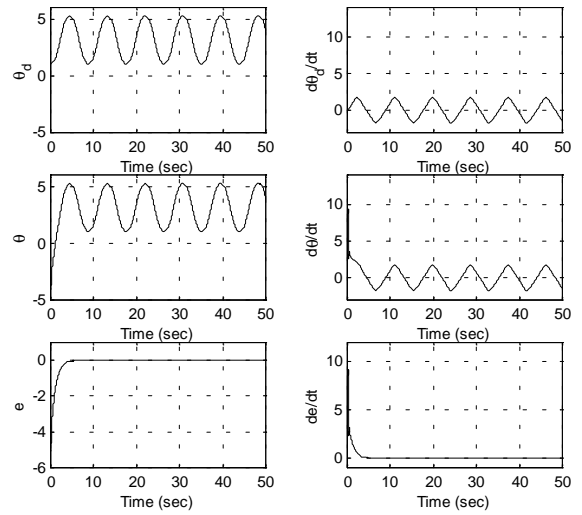


Figure 9. Desired and observed states with error signals in control of Duffing oscillator

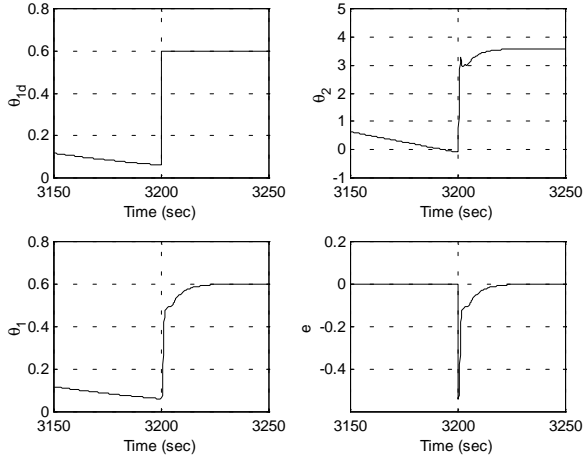


Figure 7. Zoomed Figure 5 around $t=3200$ sec.

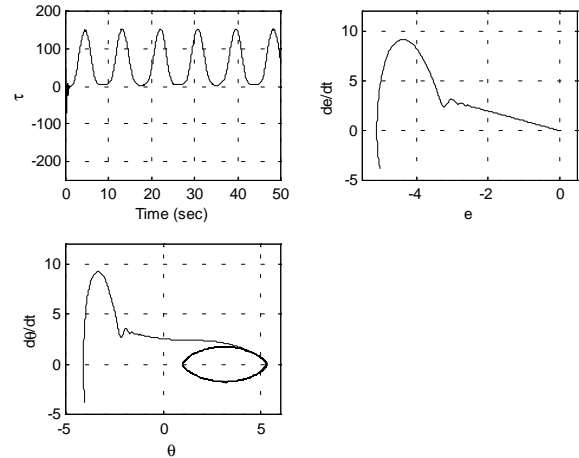


Figure 10. Applied control signal, phase space motion and state space motion

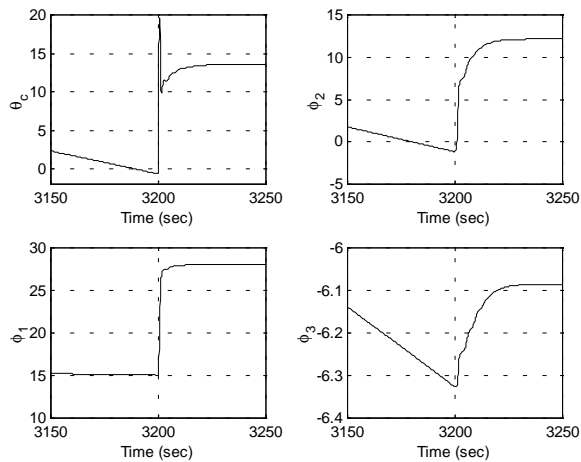


Figure 8. Zoomed Figure 6 around $t=3200$ sec.

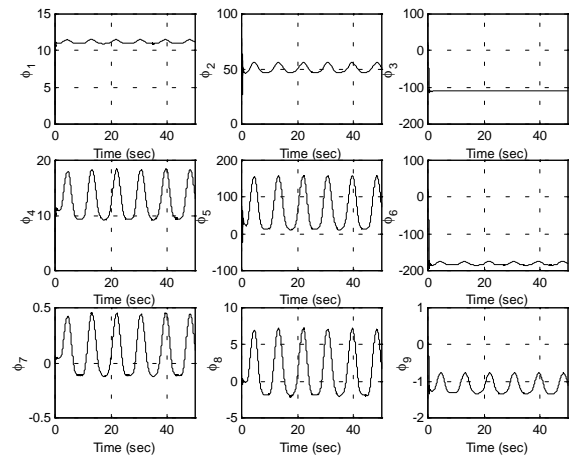


Figure 11. Time evolution of the RBFNN controller parameters

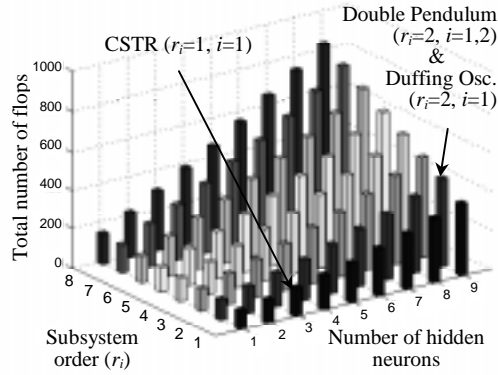


Figure 12. Computational complexity chart

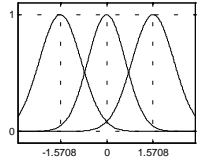
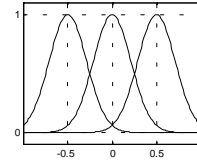
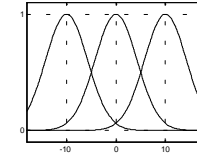
Table I. Parameters of the Double Pendulum

Mass of pendulum 1	M_1	2 kg
Mass of pendulum 2	M_2	2.5 kg
Mom. of inertia for pend. 1	J_1	0.5 kg
Mom. of inertia for pend. 2	J_2	0.625 kg
Spring constant	k_s	100 N/m
Natural length of the spring	l	0.5 m
Distance btw. pend. hinges	b	0.4 m
Pendulum height	r	0.5 m

Table III. Parameters of the CSTR Dynamics

Dimensionless concentration	θ_1	State variable
Dimensionless temperature	θ_2	State variable
Dimensionless coolant temp.	θ_c	Control input
Damkohler number	Da	0.072
Dimensionless cooling rate	β	0.3
Dimensionless activation energy	γ	20
Dimensionless heat of reaction	T_R	1
Disturbance	η	See Table II

Table II. Simulation Data for the Examples

	Double Pendulum	CSTR	Duffing Oscillator
Controller Input Vector	$u_i = [e_i \quad \dot{e}_i]^T, i=1,2$	$u_i = e_i, i=1$	$u_i = [e_i \quad \dot{e}_i]^T, i=1$
# of Hidden Neurons	9 for each RBFNN	3	9
Uncertainty Bounds	$k_1=1000, k_2=1000$	$k=20$	$k=1000$
Simulation Stepsize	$T_s=2.5\text{msec}$	$T_s=0.1\text{sec}$	$T_s=2.5\text{msec}$
Initial Errors	$e_1(0)=5\pi/12$ rad $e_2(0)=-\pi/2$ rad $\dot{e}_1(0)=0$ rad/sec $\dot{e}_2(0)=0$ rad/sec	$e(0)=-0.0566$	$e(0)=-5$ $\dot{e}(0)=-4$
Sliding Line Parameter	$\lambda_1=1, \lambda_2=1$	None	$\lambda=1$
Noise Variance	$0.33e-6$	$7.3543e-8$	$0.75e-7$
Noise Peak Value with probability ≈ 1	$1e-3$	$1e-3$	$1.5e-3$
SMC Design Matrix	$\xi = I_{2 \times 2}$	$\xi = 0.1I_{1 \times 1}$	$\xi = I_{1 \times 1}$
Filtering Parameter	$\alpha=100$	$\alpha=1$	$\alpha=1$
Initialization of the Basis Functions, which are kept static during the simulations	 e_i or de_i/dt	 e_i	 e_i or de_i/dt